http://dx.doi.org/10.5012/bkcs.2012.33.3.1078

Preferential Evolution of Prussian Blue's Morphology from Cube to Hexapod†

Seung-Hyun Lee and Young-Duk Huh*

Department of Chemistry, Institute of Nanosensor and Biotechnology, Dankook University, Gyeonggi-Do 448-701, Korea
**E-mail: ydhuh@dankook.ac.kr*
Received December 19, 2011, Accepted January 13, 2012

Key Words : Prussian blue, Morphology evolution, Preferential etching

Prussian blue (PB), $Fe_4^{3+}[Fe^{2+}(CN)_6]_3 \cdot xH_2O$, has been used as a pigment for three centuries.[1] It has a prototypical haxacyanometallic face centered cubic structure, with the Fe^{3+} coordinating the nitrogen atoms and the Fe^{2+} to the carbon, resulting in Fe^{3+}–NC–Fe^{2+}–CN–Fe^{3+} linkage.[2] The separation between the Fe^{3+} ions corresponds to an $a = 1.031$ nm. A similar compound, soluble Prussian blue, ($KFe^{3+}[Fe^{2+}(CN)_6]$) contains potassium ions in alternate interstitial sites (Scheme 1).

PB analogues have unique and potentially useful magnetic, optical, and structural properties. Photoinduced magnetization has been observed in $K_{0.2}Co_{1.4}[Fe(CN)_6]\cdot 9H_2O$, a PB analogue.[3] Incident light can induce electrons to transfer from Fe^{2+} (S=0) to Co^{3+} (S=0) in the Fe^{2+}–CN–Co^{3+} linkage, yielding a long-lived metastable Fe^{3+}–CN–Co^{2+} linkage with Fe^{3+} (S=1/2) to Co^{2+} (S=3/2), resulting in photo-induced magnetization. Therefore, PB analogues have been studied as photoinduced magnets and molecular magnets and photomagnetic switches.[4-9] They have porous frameworks and contain water molecules at the incomplete coordination sites at the surfaces of their frameworks. The coordinated water molecules can be removed by moderate heating and hydrogen gas can be stored in the resulting spaces, making PB analogues potential useful for hydrogen storage.[10-12] They can also act as electrocatalysts for both the reduction and oxidation of hydrogen peroxide and as sensors of hydrogen peroxide and biological glucose.[13-15]

Controlling PB analogues' morphology during their synthesis is important as it affect their properties.[16-20] PB analogues have face centered cubic structures, leading to most PB analogues showing cubic morphologies.[21-23] Most synthetic methods have aimed to prepare a single final morphology and relatively little is known about the morphology evolution of PB analogues with respect to the synthetic conditions. To the best of authors' knowledge, this is the first report of the evolution of PB's morphology from cube to hexapod.

Figure 1 shows X-ray diffraction (XRD) patterns of PB products prepared by microwave-assisted reactions from aqueous $K_4[Fe^{2+}(CN)_6]$ using different concentrations of HNO_3. When 8.0×10^{-2} M HNO_3 was used, XRD patterns resulted in peaks attributable to only $KFe^{3+}[Fe^{2+}(CN)_6]$,

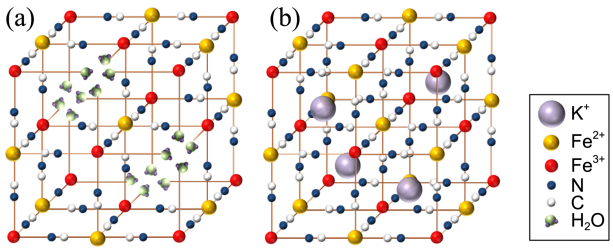

Scheme 1. The crystal structures of (a) $Fe_4^{3+}[Fe^{2+}(CN)_6]_3 \cdot xH_2O$ (insoluble Prussian blue) and (b) $KFe^{3+}[Fe^{2+}(CN)_6]$ (soluble Prussian blue).

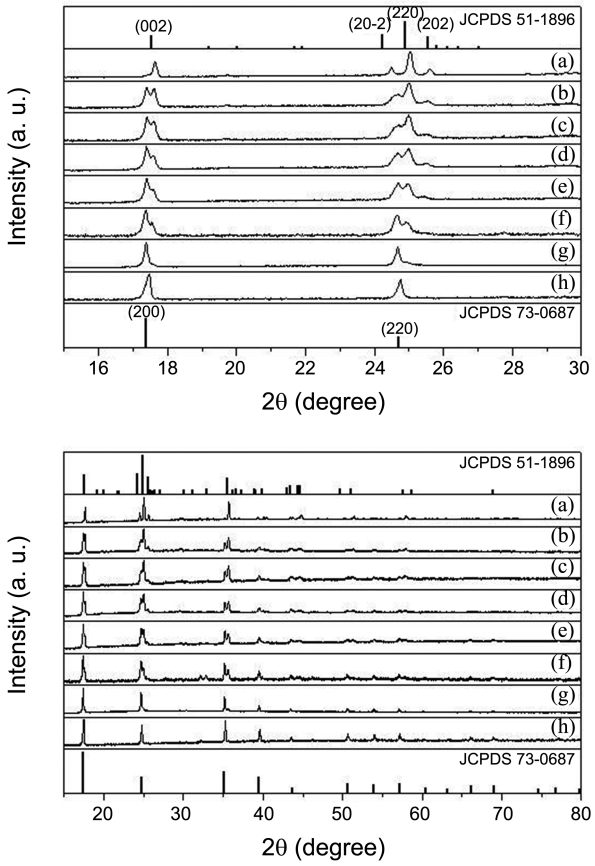

Figure 1. Powder XRD patterns of Prussian blue prepared with different concentrations of HNO_3 over ranges of 2θ intervals of (top) 15°-30° and (bottom) 15°-80°: (a) 8.0×10^{-2} M, (b) 1.6×10^{-1} M, (c) 2.0×10^{-1} M, (d) 2.4×10^{-1} M, (e) 3.4×10^{-1} M, (f) 3.9×10^{-1} M, (g) 4.8×10^{-1} M, and (h) 5.7×10^{-1} M.

†This paper is to commemorate Professor Kook Joe Shin's honourable retirement.

soluble PB. XRD data of $KFe^{3+}[Fe^{2+}(CN)_6]$ are not available and results were compared to the similar structure of monoclinic $KMn^{3+}[Fe^{2+}(CN)_6]$ (JCPDS 51-1896, a = 1.0108 nm, b = 1.0104 nm, c = 1.0114 nm, β = 92.93°). Since the ionic radius of Fe^{3+} (0.64 Å) is slightly smaller than that of Mn^{3+} (0.66 Å), the XRD peaks of $KFe^{3+}[Fe^{2+}(CN)_6]$ appeared at slightly higher angles than those of $KMn^{3+}[Fe^{2+}(CN)_6]$.[24] Increasing the use HNO_3 to 5.7×10^{-1} M resulted in peaks attributable to only cubic PB, $Fe_4^{3+}[Fe^{2+}(CN)_6]_3 \cdot xH_2O$, (JCPDS 73-0687, a = 1.031 nm). Using HNO_3 at 1.6×10^{-1} – 4.8×10^{-1} M, led to XRD peaks attributable to both PB and soluble PB. Increasing use of HNO_3, increased the intensity of the peak attributable to insoluble PB at 17.46° and decreased that attributable to soluble PB at 17.62° (Figure 1). This indicates that soluble PB was converted to insoluble PB as the concentration of HNO_3 increased. The FT-IR spectra of soluble PB and insoluble PB showed the very strong peaks at 2065 cm^{-1}, which are corresponded stretching vibration of CN. The energy-dispersive X-ray spectroscopy (EDS) was also used to further characterize the compositions of soluble PB and insoluble PB. The EDX data within experimental errors also confirmed that the soluble PB and insoluble PB had been synthesized. [Analysis observed (calculated) for soluble PB: C, 31.6 (40.0%); N, 42.4 (40.0%); K, 12.3 (6.7%); Fe, 13.7 (13.3%); O, 0.0 (0.0%) and for insoluble PB of $Fe_4^{3+}[Fe^{2+}(CN)_6]_3 \cdot 17H_2O$: C, 35.4 (30.0%); N, 38.7 (30.0%); K, 3.0 (0.0%); Fe, 9.1 (11.7%); O, 13.8 (28.3%)].

Aqueous $K_4[Fe^{2+}(CN)_6]$ was used with HNO_3 to prepare soluble PB and insoluble PB under microwave irradiation. The formation constant of $[Fe^{2+}(CN)_6]^{4-}$ at 25 °C is *ca.* 1×10^{37}. Under microwave irradiation, $[Fe^{2+}(CN)_6]^{4-}$ dissociated slowly into Fe^{2+} ions. $[Fe^{2+}(CN)_6]^{4-}$ was also partially oxidized by HNO_3 and then Fe^{3+} ions were released. The Fe^{3+} ions reacted with $[Fe^{2+}(CN)_6]^{4-}$ to produce soluble PB, $KFe^{3+}[Fe^{2+}(CN)_6]$. K^+ ions were further substituted by Fe^{3+} ions to form insoluble PB, $Fe_4^{3+}[Fe^{2+}(CN)_6]_3 \cdot xH_2O$.

The PB products prepared with local thermal heating under microwave irradiation from aqueous $K_4[Fe^{2+}(CN)_6]$ and different concentrations of HNO_3 were characterized by scanning electron microscopy (SEM), as shown in Figure 2. 8.0×10^{-2} M HNO_3 led to the formation of soluble PB. 1.6×10^{-1} M and 2.0×10^{-1} M HNO_3 resulted in truncated cubes, the corners of which were etched by the acid. Increasing the concentration of HNO_3, transformed the truncated cubes to

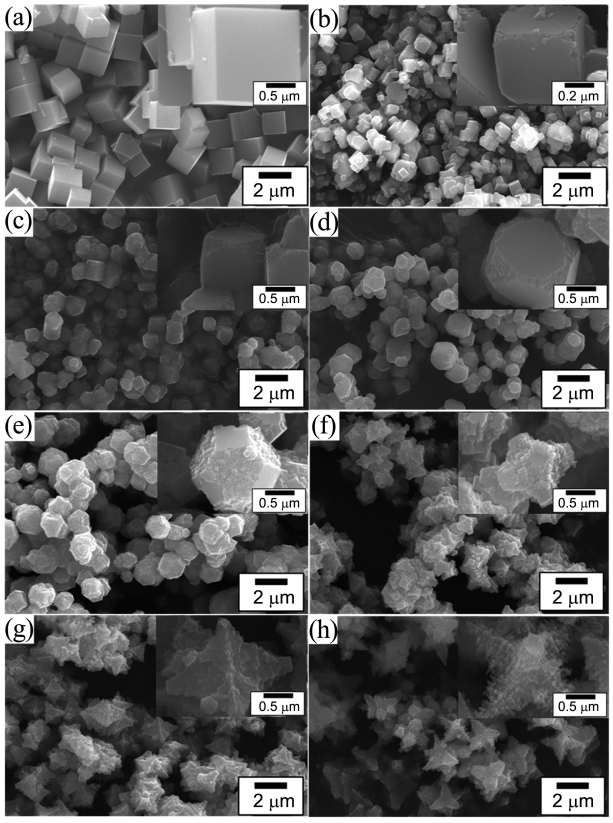

Figure 2. SEM images of Prussian blue prepared with different concentrations of HNO_3: (a) 8.0×10^{-2} M, (b) 1.6×10^{-1} M, (c) 2.0×10^{-1} M, (d) 2.4×10^{-1} M, (e) 3.4×10^{-1} M, (f) 3.9×10^{-1} M, (g) 4.8×10^{-1} M, and (h) 5.7×10^{-1} M.

cuboctahedrons and then to truncated octahedrons. 3.9×10^{-1} M HNO_3 resulted in hexapods with six arms. Further increases of HNO_3 to 4.8×10^{-1} M and 5.7×10^{-1} M etched the arms of hexapods to form star-like hexapods.

PB's morphological evolution with increasing HNO_3 concentration is outlined in Figure 3. As increasing HNO_3 concentration, the particles evolved from cubes, through truncated cubes, cuboctahedrons, truncated octahedrons, and hexapods with arms, to star-like hexapods. This indicates that the oxidation reaction started at the cubes' corners, suggesting that the rate of etching at the {111} planes was much faster than at the {100} planes. The truncated cubes formed through etching at the corners of the cubes of soluble PB. Increasing the concentration of HNO_3 increased the

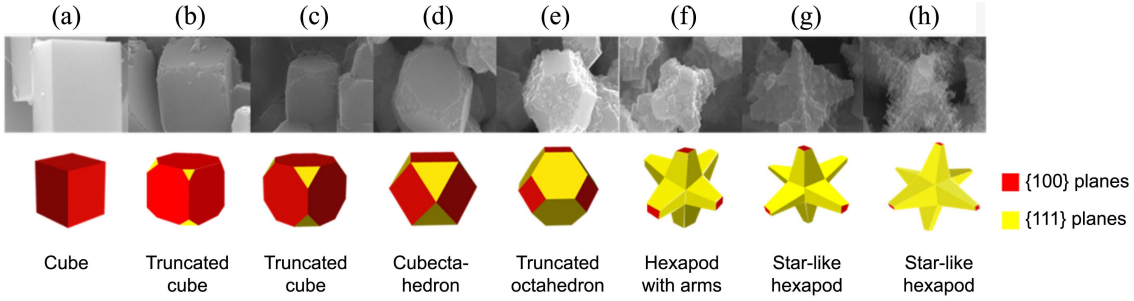

Figure 3. Morphology evolution of the Prussian blue from cube to star-like hexapod with increasing concentrations of HNO_3.

etched areas at the cubes' corners, leading them to being etched into cuboctahedrons and truncated octahedrons. Star-like hexapods were then obtained by etching almost all of the {111} planes and some of the {100} planes. Therefore, the morphology of crystal of the soluble PB, $KFe^{3+}[Fe^{2+}(CN)_6]$, evolved from cubes to the star-like hexapods of insoluble PB, $Fe_4^{3+}[Fe^{2+}(CN)_6]_3 \cdot xH_2O$, *via* the other shapes by increasing the reaction rate along the {111} planes with increased amounts of HNO_3.

The morphologies of PB particles formed under microwave irradiation by the reaction of $K_4[Fe^{2+}(CN)_6]$ depended upon the concentration of HNO_3. Etching with HNO_3 was important in determining the morphology, as the etching reaction occurred preferentially along the {111} planes of the PB structures.

Experimental Section

$K_4[Fe(CN)_6]$ (Aldrich, 98.5%) and HNO_3 (Aldrich, 69%) were used as received. For the synthesis of soluble PB, 2.0 mmol $K_4[Fe(CN)_6]$ was dissolved in 100 mL distilled water and 0.6 mL HNO_3 (8.0×10^{-2} M) was added under stirring for 5 min. The mixed solution was irradiated in a domestic microwave oven (Amana M84T, 2.45 GHz, 25 W) for 3 min. The oven was operated in cycles of 30 s – on and 30 s – off to minimize solvent superheating. The effects of HNO_3 on the PB's morphology were tested using HNO_3 at 8.0×10^{-2} M, 1.6×10^{-1} M, 2.0×10^{-1} M, 2.4×10^{-1} M, 3.4×10^{-1} M, 3.9×10^{-1} M, 4.8×10^{-1} M, and 5.7×10^{-1} M, with all other conditions kept constant. The products were obtained by centrifuging at 4000 rpm for 5 min, repeated washing with ethanol and water, and drying at 60 °C for 24 h.

Products' structures were analyzed by powder X-ray diffraction (XRD, PANalytical, X'pert-proMPD) using Cu Kα radiation. Their morphologies were characterized by scanning electron microscopy (SEM, Hitachi S-4300) equipped with an energy-dispersive X-ray spectroscopy (EDS) operating at an accelerating voltage of at 15 kV. The FT-IR spectra were obtained using a Perkin-Elmer Spectrum 100 FT-IR spectrometer in the attenuated total reflectance (ATR) mode over the range 650-4000 cm^{-1} at a resolution of 4 cm^{-1}.

References

1. Robin, M. B. *Inorg. Chem.* **1962**, *1*, 337.
2. Buser, H. J.; Schwarzenbach, D.; Petter, W.; Ludi, A. *Inorg. Chem.* **1977**, *16*, 2704.
3. Sato, O.; Iyoda, T.; Fujishima, A.; Hashimoto, K. *Science* **1996**, *272*, 704.
4. Pajerowski, D. M.; Gardner, J. E.; Frye, F. A.; Andrus, M. J.; Dumont, M. F.; Knowles, E. S.; Meisel, M. W.; Tallham, D. R. *Chem. Mater.* **2011**, *23*, 3045.
5. Culp, J. T.; Park, J. H.; Frye, F.; Huh, Y. D.; Meisel, M. W.; Talham, D. R. *Coord. Chem. Rev.* **2005**, *249*, 2642.
6. Pajerowski, D. M.; Gardner, J. E.; Talham, D. R.; Meisel, M. W. *J. Am. Chem. Soc.* **2009**, *131*, 12927.
7. Bleuzen, A.; Lomenech, C.; Escax, V.; Villain, F.; Varret, F.; Moulin, C. C. D.; Verdaguer, M. *J. Am. Chem. Soc*. **2000**, *122*, 6648.
8. Liu, H. W.; Matsuda, K.; Gu, Z. Z.; Takahashi, K.; Cui, A. L.; Nakajima, R.; Fujishima, A.; Sato, O. *Phys. Rev. Lett.* **2003**, *90*, 167403.
9. Tokoro, H.; Ohkoshi, S. I. *Dalton Trans*. **2011**, *40*, 6825.
10. Chapman, K. W.; Southon, P. D.; Weeks, C. L.; Kepert, C. J. *Chem. Commun.* **2005**, 3322.
11. Jiménez-Gallegos, J.; Rodríguez-Hernández, J.; Yee-Madeira, H.; Reguera, E. *J. Phys. Chem. C* **2010**, *114*, 5043.
12. Kaye, S. S.; Long, J. R. *J. Am. Chem. Soc.* **2005**, *127*, 6506.
13. de Tacconi, N. R.; Rajeshwar, K. *Chem. Mater.* **2003**, *15*, 3046.
14. Koncki, R.; Lenarczuk, T.; Radomska, A.; Glab, S. *Analyst* **2001**, *126*, 1080.
15. Ricci, F.; Palleschi, G. *Biosens. Bioelectron.* **2005**, *21*, 389.
16. Sun, H. L.; Shi, H.; Zhao, F.; Qi, L.; Gao, S. *Chem. Commun.* **2005**, 4339.
17. Cao, M.; Wu, X.; He, X.; Hu, C. *Chem. Commun.* **2005**, 2241.
18. Shen, X.; Wu, S.; Liu, Y.; Wang, K.; Xu, Z.; Liu, W. *J. Colloid Interface Sci.* **2009**, *329*, 188.
19. Xu, S.; Qian, X.; Li, G. *Mater. Res. Bull.* **2008**, *43*, 135.
20. Hu, M.; Jiang, J. S; Ji, R. P.; Zeng, Y. *CrystEngComm* **2009**, *11*, 2257.
21. Yang, J.; Wang, H.; Lu, L.; Shi, W.; Zhang, H. *Cryst. Growth Des.* **2006**, *6*, 2438.
22. Hu, M.; Jiang, J. S. *Mater. Res. Bull.* **2011**, *46*, 702.
23. Vaucher, S.; Li, M.; Mann, S. *Angew. Chem. Int. Ed.* **2000**, *39*, 1793.
24. Weast, R. C. *Handbook of Chemistry and Physics*, 70th ed.; 1989; F-187.